

The Electrochemical Behaviour of 70-30 Cu-Ni Alloy in LiBr Solutions

A.A. El Warraky, A. E. El Meleigy and Sh. E. Abd El Hamid

Department of Physical Chemistry, N. R. C., Dokki, Giza, PO 12622, Egypt.

THE BEHAVIOUR of 70-30Cu-Ni alloy has been investigated in different concentrations of LiBr solutions from 10^{-1} to 9 M. Electrochemical measurements and surface examination complemented with solution analysis were carried out. The results revealed that the passivation current of (I_{p1}) at low anodic potential (-200) is due to the formation of a doped Cu_2O film involving surface enrichment of nickel. Increasing the anodic potential to ≥ 300 mV, after the formation of a peak of anodic current maximum (I_{p2}) a partially passive film of $Cu_2(OH)_3Br$ is formed and the surface suffered from denickelification.

Furthermore, solution analysis proves that the alloy dissolves showing a copper/ nickel ratio in solution which approximation complete that of the alloy surface. Two types of pitting corrosion were recorded at 2 and 4 M LiBr, the first one was recorded after I_{p1} while the second is recorded after +1000mV. Except the concentration of 2 and 4 M the first one only of pitting which recorded after I_{p1} were observed beside the general dissolution through the partially soluble $Cu_2(OH)_3Br$.

Keywords: Copper -Nickel, LiBr, Denickelification, Pitting corrosion and general dissolution.

Cu/Ni alloys are used in absorption machines because of their high thermal conductivity, good mechanical properties and excellent corrosion resistance in aqueous solutions. Cu/Ni alloys are the most important one of the main alloys used for the construction of absorption chillier. They are used in the construction of heat exchangers condenser in lithium bromide (LiBr) absorption machines. LiBr heavy brain is widely used as absorbents for almost all type of heating and refrigerating absorption systems⁽¹⁻⁸⁾.

Recent studies were conducted to investigate the corrosion behaviour of copper in LiBr solution up to 9 M. The electrochemical results⁽⁹⁾ and surface examination⁽⁸⁾ of that work show that, in diluted solutions, $\leq 4 \times 10^{-2}$ M, general dissolution takes place. As the concentration of LiBr increased up to 7×10^{-1} M passive film of CuO and Cu(OH) appeared and pitting corrosion became favourable. At higher concentrations from 2 to 9 M the film formed is more

porous and not protective where general dissolution takes place through the complexing formation of soluble CuBr_2^- .

On the other hand, it is well known that, the dissolution of binary alloys containing noble metals such as Ni in Cu/Ni alloy follows a common type of corrosion which is called dealloying.

Dealloying of Cu/Ni alloy which is called denickelification, is a corrosion process in which the less noble constituent of the alloy (Ni) is preferentially removed leaving surface rich in the more noble metal (Cu). Dezincification of brass is the most common example of dealloying, the dezincification of brass has been studied in previous works by the same author⁽¹⁰⁻¹⁴⁾.

The present study was undertaken to investigate the electrochemical behaviour of Cu/30Ni in different concentrations of LiBr from 10^{-1} to 9M to clarify the different types of corrosion present. For this work potentiodynamic cyclic polarization and potentiostatic current- time measurements were used. After that scanning electron microscope (SEM) equipped with energy dispersive X-ray (EDX) was used to follow the changes which occurred on the surface of the alloy after electrochemical treatments.

Furthermore, analysis of the solutions in which the specimens were maintained at various potentials for 120 min. was performed to show the weight percentage of Cu and Ni.

Experimental

The working electrodes were made from Cu/30Ni rods and were welded to thick Cu wires for electrical connections. The welding and the Cu connection were enclosed in tight-fitting Pyrex –glass tubing, and were sealed by a neutral epoxy. The electrodes having a surface area of 1cm^2 to be contact with test solutions. All tests were carried out at room temperature and all solutions were prepared from reagent grade and bidistilled water.

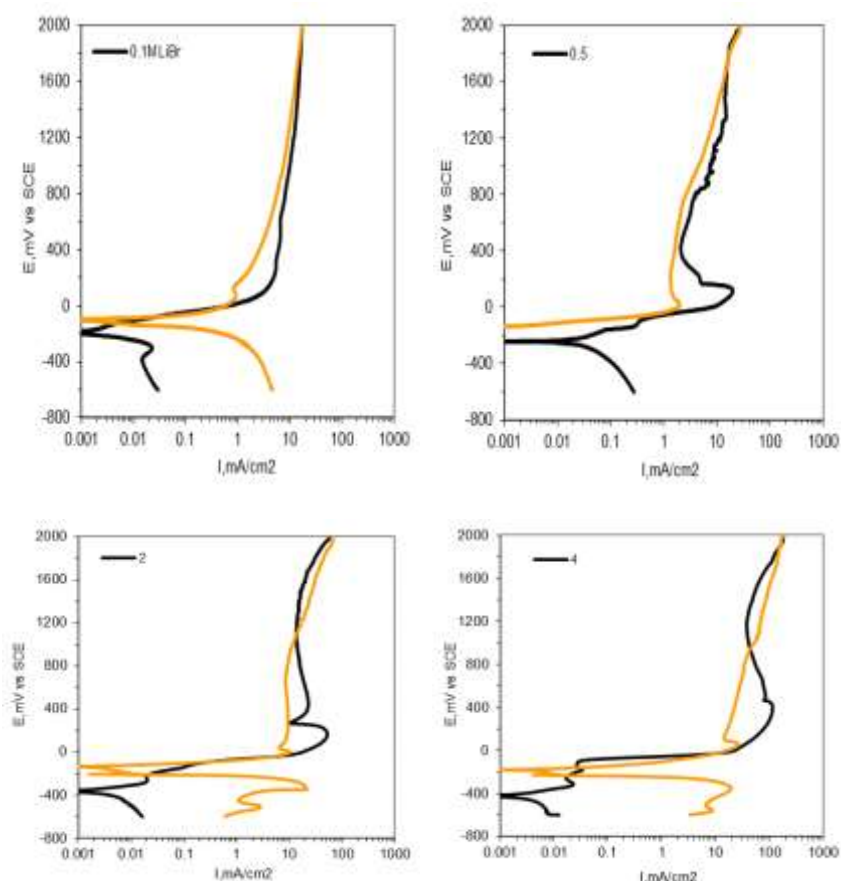
Details of the electrode surface pretreatment, solution preparation, electrochemical measurements, surface analysis techniques and other experimental methods were described previously⁽⁸⁾.

At the end of each experiment, the solutions, in which specimens were maintained to 120 min at different potentials, were analysed to show the concentrations of both Cu and Ni using the Perkin-Elmer type 2380 atomic absorption spectrophotometer technique (A.A.S).

Discussion

The potentiodynamic cyclic polarization (PCP) curves of Cu/30Ni in different concentration of LiBr from 10^{-1} up to 9 M are shown in Fig 1. The

curves exhibit an anodic passivation current at (I_{p1}) and anodic current maximum at (I_{max}). I_{p1} is observed at low noble potentials with low current densities while I_{max} was recorded at more anodic potentials and the higher current densities depend on the concentration of LiBr. The anodic polarization behaviour of Fig. 1 recorded that, in all cases the initial active region is followed by passivation behaviour and one anodic current peak is observed. This peak is followed at more anodic potentials by a small decrease in the current density. At both of 2M and 4M LiBr, hysteresis loop area is recorded at high anodic potentials (1250) and more current densities are produced. These are attributed to localized attack as a result of accumulation of the corrosion product. Previous studies by the same authors on Cu and Al-bronze^(6,10-14) showed that this peak is usually followed by a second peak. They suggest that the first peak which is denoted in this study by I_{p2} , is associated with oxidation of copper to Cu^+ and the second peak, which is not recorded in the present study, is associated with oxidation of Cu^+ to Cu^{++} state.



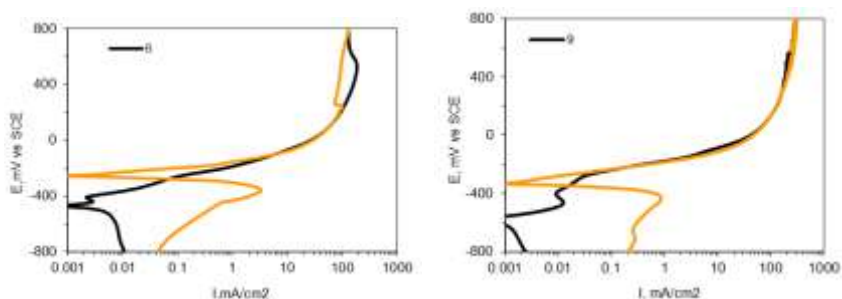


Fig.1. The potentiodynamic cyclic polarization (PCP) curves of Cu/30Ni in different concentrations of LiBr (M).

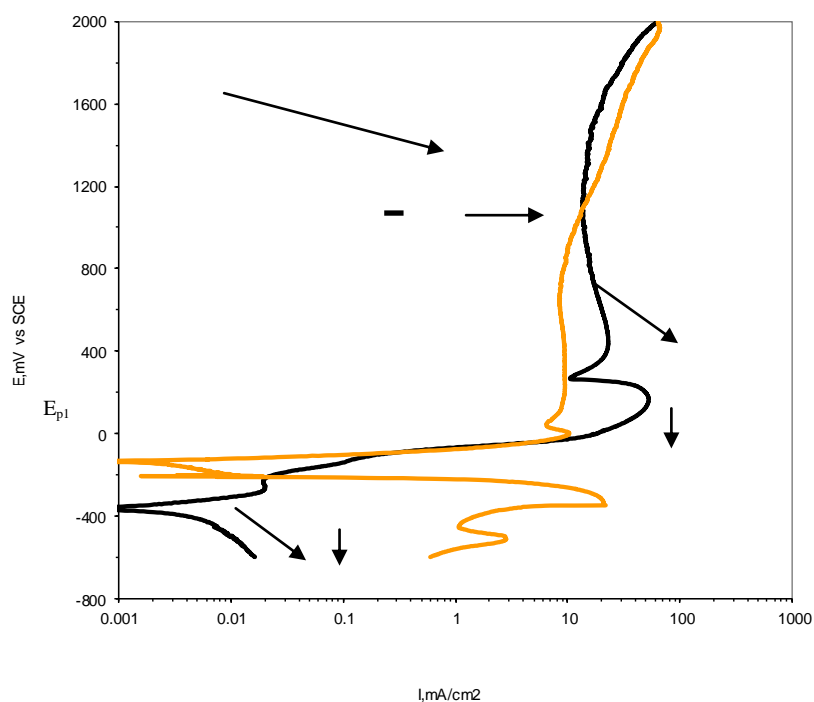


Fig.1. Continue, PCP curve of Cu/30Ni in 2M LiBr was repeated with a higher magnification to clarify the abbreviation of the important symbols.

On the other hand, as the concentration of LiBr was increased, I_{p1} shifted to more negative value and I_{max} attained higher values (Table 1). The important feature recorded in the present study which is not recorded previously^(1,6-9) is the detection of the anodic passive current at I_{p1} . Figure 2 shows corresponding typical Tafel region of the PCP curves of Fig. 1 which was taken using enlarged scale to clarify the region of the passive film recorded. By increasing the concentration from 10^{-1} to 9M, E_{corr} and the length of the passive region are

Egypt. J. Chem. **59**, No. 5 (2016)

increased, (Table 1) which reflects that the film formed became more resistance as confirmed later.

TABLE 1. Corrosion potential (E_0), Potential of anodic current maximum (E_{Max}), the first breakdown potential after passivation current (E_{P1}), the second breakdown potential after partially passivation current (E_{P2}), anodic passivation current (I_{P1}), anodic current maximum (I_{Max}), the length of the passive region $E_{P1} - E_0$ for PCP of Cu/30Ni alloy in 2M LiBr at room temp.

Conc.	E_0	E_{P1}	$E_{P1} - E_0$	E_{Max}	E_{P2}	I_{P1}	I_{Max}
10^{-1}	-200	-----	200	260	-----	-----	5.42
5×10^{-1}	-250	-100	150	150	-----	0.34	15.60
2	-390	-210	180	220	1600	0.02	43.54
4	-420	-160	260	365	1350	0.0288	113.53
6	-480	-400	80	570	-----	0.0025	177.385
9	-600	-380	220	245	580	0.01	147.12

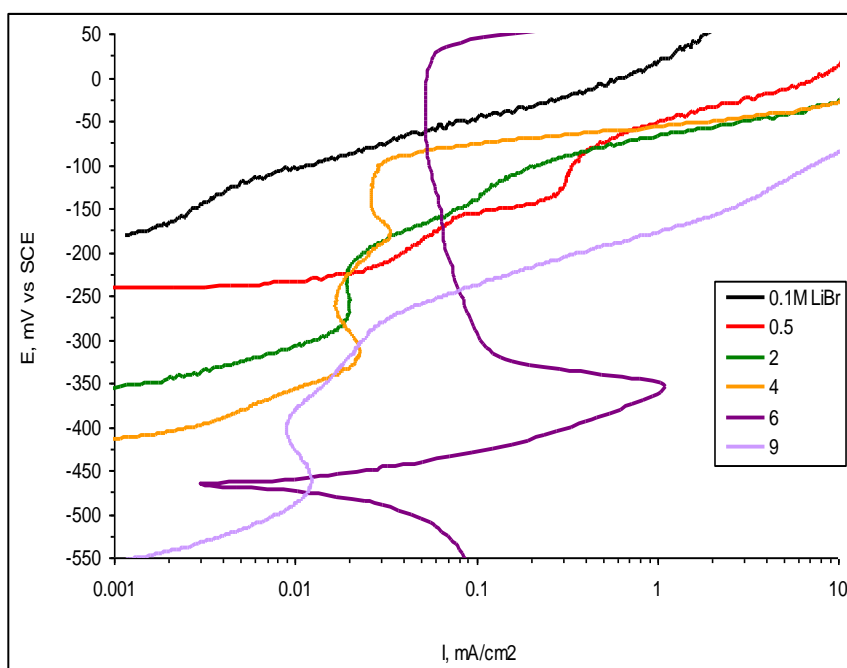


Fig.2. The length of anodic passivation current (I_{P1}) of Cu/30Ni in xM LiBr.

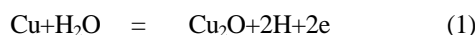
In the light of the above studies, it was necessary to use current-time measurements at various constant potentials, in combination with the surface

examination by SEM and EDX, can give clear information about the behaviour of Cu/30Ni in 2M LiBr solutions. In this instance, a concentration of 2 M LiBr was selected because it was intermediate and had no higher dissolution current. Figure 3 presents the measurements of the current density against time for the test coupon kept for 120 min at different anodic potentials of -200, +300 and +1600 mV in 2M LiBr.

Important features are recorded:

(1) At -200 mV, through I_{p1}

The initial current density begins at very small values which slightly decrease and a steady –state value was found to reach 0.01 mA within less than 20 min as shown in Fig. 3(a). Examination of the surface of the treated sample at the end of experiment is shown in Fig. 4 (a). The micrograph of Fig. 4(a) clearly shows that there is no any attack and the surface is covered with a regular extended film. An important feature in both polarization curve of Fig. 2 and SEM of Fig.4 (a) is reinforced by surface analysis by EDX of Fig. 4 (b) and Table 2(a) confirms that the film formed is more passive and shows a higher at. % which reached 62%. This confirms that the anodic passivation region (I_{p1}) corresponds to the formation of Cu_2O as follows ^(1,6-9,16-19):

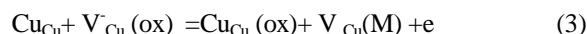


Several authors have confirmed that the passivation in chloride solutions is established during the initial anodic polarization by the formation of P-type semiconductor which can accept different foreign ions such as Ni ⁽²⁰⁻²⁴⁾, iron ^(20,25,26) or chloride ⁽²²⁻²⁴⁾. The formation of Cu_2O on the alloy surface as a result of the inward transport of Br ion and outward diffusion of metallic ion.

The migration of Cu^+ away from the alloy surface would create cation vacancies ^(20,27).

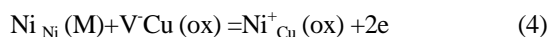


where $Cu^+(aq)$ is a positively charged Cu^+ site in the film and $V_{Cu}^-(ox)$ is a negatively charged cation vacancy



where $V_{Cu}(M)$ is a neutral vacancy generated by the copper cation in the alloy.

After the dissolution potential of Ni, Ni^{2+} occupies the cation vacancies as



where $Ni_{Cu}(ox)$ is a positively charged Ni^{2+} that occupies the vacancy generated by Cu_2O and $Ni_{Ni}(M)$ is a nickel atom in a metal. Accordingly, Ni from the alloy segregated to the semiconducting Cu_2O through the solid state reaction to occupy

the mobile cation vacancies and result in a vacancy with a positive charge. This would electrostatically interact with Ni^{2+} which leads to decreasing the ionic conductivity and increasing the electronic conductivity of Cu_2O which reflects an increase in the corrosion resistance of the alloy as recorded previously in case of NaCl solution⁽¹⁶⁻¹⁹⁾.

It was possible from the above to confirm the contribution of Ni in increasing the passivation of Cu_2O where, Fig 4(b) and Table 2 (a) show that the at. % was Cu 22.33 and Ni 44.6 and its ratio in the surface film reached 1.5% compared to the alloy bulk composition of Cu70/Ni30 where its ratio is 2.25%. This confirmed that at I_{p1} in general, resulted in higher surface Ni, enrichment of Ni on the surface. The decreased detection of Cu reflects the larger screening effect of the relatively larger accumulation of the more resistance insoluble Cu_2O on Cu sites than NiO does on Ni sites.

As increasing the polarization after -200 as in Fig. 2 would generate nickel ions which increase the ratio of incorporated NiO on the surface until a critical value. Above this value, the film formed becomes less resistant^(16-19,27). This occurs where the incorporated Ni consumes nearly all the mobile cation vacancies in Cu_2O . Increasing the Ni leads to the formation of a barrier layer of NiO on the surface which is less resistant than the doped Cu_2O layer. Further polarization as in Fig. 2 the passive film is followed by the breakdown in the potential (E_{p1}) depending on the concentration of LiBr.

(2) At +300 mV, after formation of I_{max} .

From the current- time curve of Fig. 3 (b), the value of the current density I (mA/cm^2) begins at higher value of 130 which is decreased rapidly to ≈ 6 and increased again to reach 34 mA. The current density decreased with time again to reach $\approx 8\text{mA}$ within 60 min which means that the surface became not barrier enough and it suffers from higher corrosion rate. Examination of the surface after this experiment is shown in the photograph of SEM of Fig. 5 (a). The image shows that the surface suffered severe general attack. From the spectra recorded in Fig. 5(b) at. % of Cu/Ni were 45.95/4.01, respectively where its ratio is 11.37% which is higher than the bulk composition ratio of 2.25% as shown in Table 2 (a). Thus a higher ratio of Cu/Ni above 2.25% would indicate the occurrence of dealloying or denicklification.

In view of the above result the preferential removal or dissolution of Ni has probably two effects : First, as increasing the anodic potential all the created vacancies are consumed by the segregated Ni ion to form a neutral species. Hence further increasing in anodic potential would generate Ni ions which cannot be consumed by the cation vacancies and leads to the formation of unprotected layer of NiO which is less resistant than the doped Cu_2O layer.^(17,27,28)

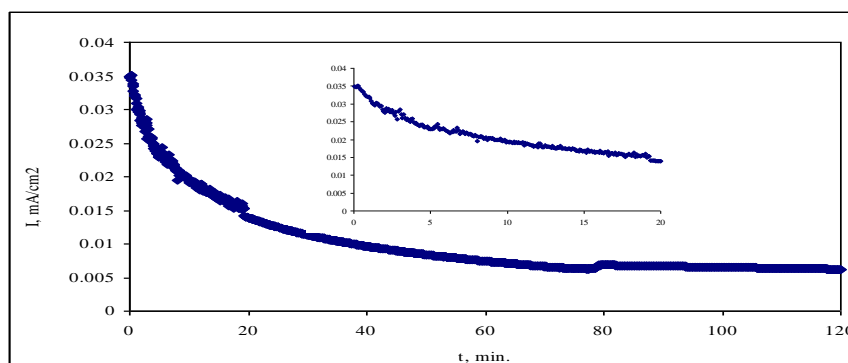


Fig.3(a)

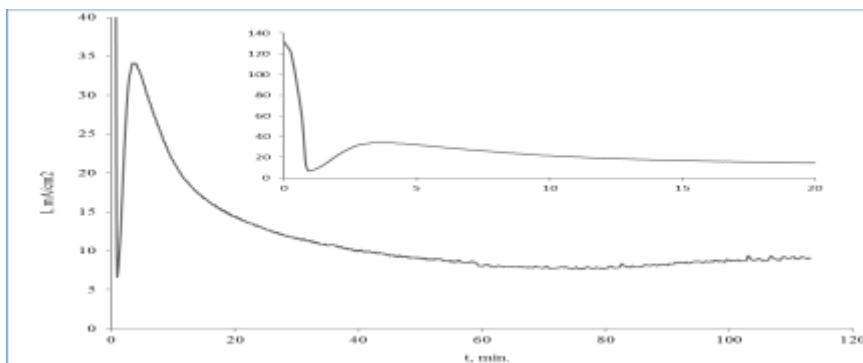


Fig.3(b)

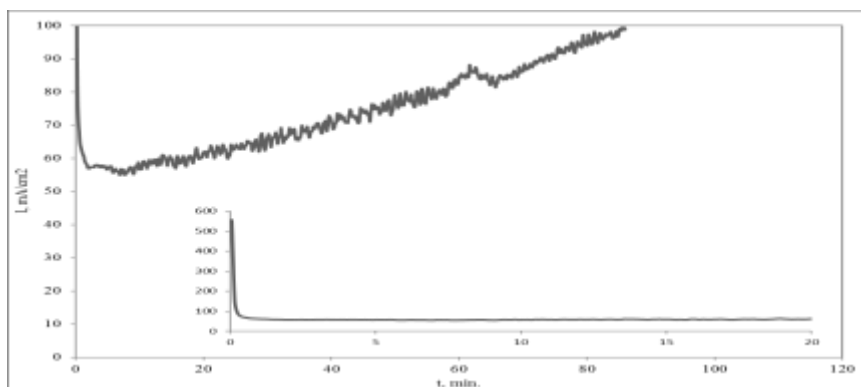


Fig.3(c)

Fig.3. Potentiostatic current-time curve for Cu/30Ni in 2M LiBr at -200 mV of applied potential

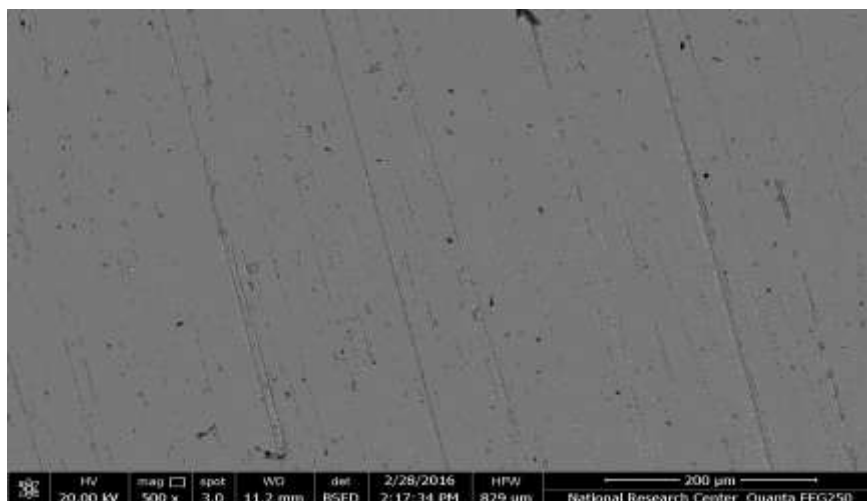


Fig. 4(a)

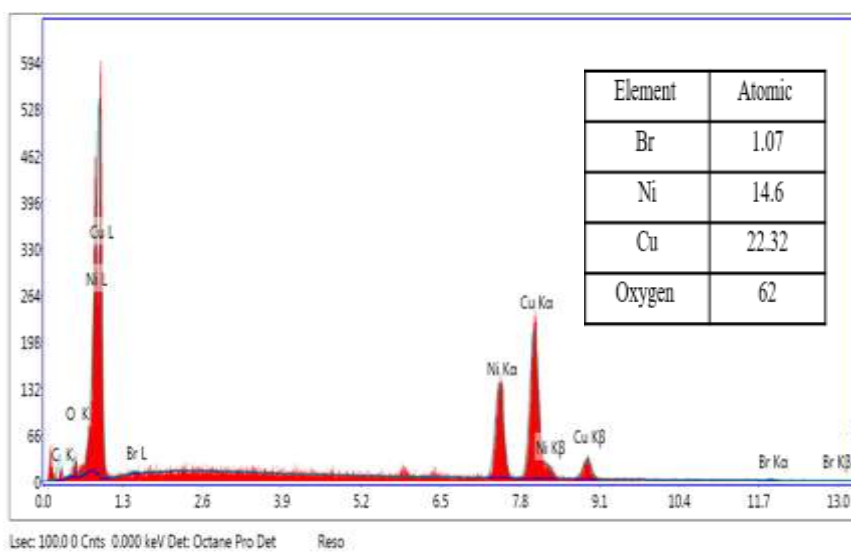


Fig. 4(b)

Fig.4. SEM micrograph of Cu/30Ni electrode obtained after Potentiostatic current-time of Fig. 3(a)

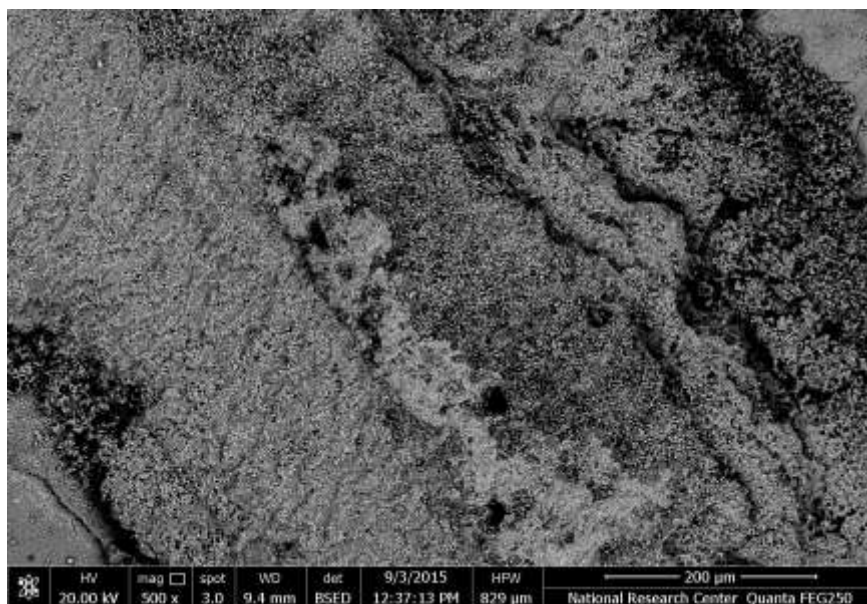


Fig. 5(a)

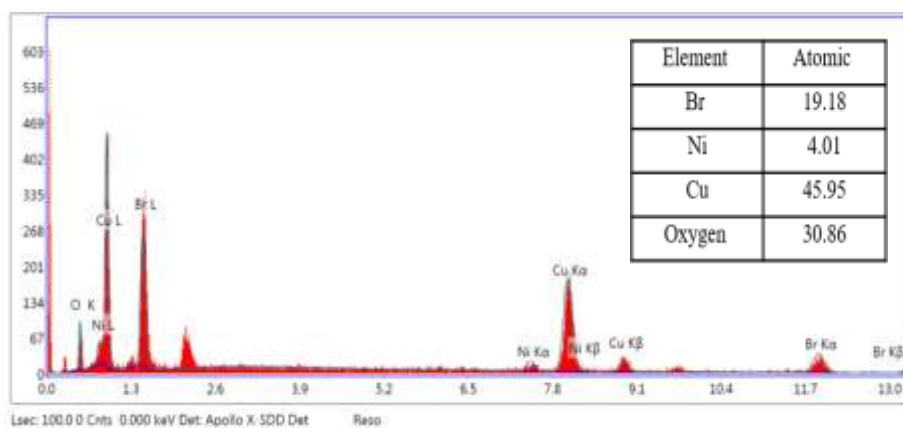


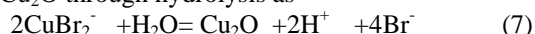
Fig. 5(b)

Fig. 5. SEM micrograph of Cu/30Ni electrode obtaining after Potentiostatic current-time of Fig. 3(b)

The second effect is related to the free corrosion potential of Cu and Ni. Previously the potentiodynamic polarization for Cu⁽⁸⁾ and Ni⁽²⁹⁾ in 2M LiBr indicates that, the free corrosion potential of Cu and Ni is -360,- 510, respectively which is in the E_{corr.} of Cu 70/30 Ni and both element are in the active region. However, the corrosion rate of Ni is at least lower magnitude than Cu by -150mV. Accordingly the breakdown in potential after E_{p1} can be interpreted by the dissolution of Ni with the formation of Ni²⁺ which leave the film to inter into the solution in the form of soluble NiBr₂ as will be confirmed later by solution analysis. Table 2 (a) confirm the dealloying of the alloy surface. Regarding to the anodic peaks formed, most authors confirmed the two peaks sequence, ^(1,6-9) where the first one is due to the oxidation of Cu to Cu⁺ and the second is the oxidation of Cu⁺ to Cu⁺⁺. It has been suggested that the dissolution at this higher concentration of LiBr is



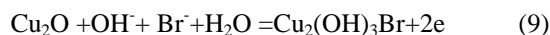
The higher concentration of CuBr₂⁻ at the metal surface leads to the formation of Cu₂O through hydrolysis as ⁽³⁰⁾



While the cathodic reaction occurs by the reduction of oxygen as



The increase of OH⁻ around the electrode surface accelerates reaction (7) and the formation of Cu₂O is responsible for the decrease in anodic current as represented by the clear peak which is formed around 300 mV as in Fig. 1. Further polarization to more anodic leads oxidation of Cu₂O and or CuBr to form a top layer of partially soluble hydroxyl bromide atacemite which is less protective.



The EDX analysis of Fig.5(b) and Table 2(a) satisfy the formation of Cu₂(OH)₃Br as in eq. (9) where the at. % were O 30.86/Br 19.18.

(3) At 1600 mV (after E_{p2})

It is worthy of mention that the PCP of Fig. 1 (c) indicate that after I_{p2} a partially passive current density is recorded and a breakdown in potential observed at 1250mV. After that an increase in the anodic current was produced and after the backward a hysteresis loop area is produced where the repassivation potential (E_{rp}) is recorded at 1180 mV. This confirmed that after 1250 mV, the surface suffered from local attack.

In the light of the above results, it was necessary to examine the surface after E_{p2} . In this instance, a potential at 1600mV was selected because it was higher than E_{p2} or the repassivation potential (E_{rp}) to clarify the type of local attack.

Fig. 3(c) shows the measurements of the current density against time at 1600mV vs SCE in 2M LiBr. As can be observed in Fig. 3(c) a higher current density of 580 mA was recorded at the first moment of polarization where a sharp decrease in the current density with time to nearly 55 mA occurred. Then a slow rate of increase in the current density with a fluctuation was recorded which extended to the end of experiment. These fluctuations were due to the formation of small pits. Examination of the surface of Fig. 6(a) using SEM confirms the above result of current-time and shows that some initiation of pits are evident over the surface which do not propagate.

The EDX analysis of Fig. 6(b) showed a higher Cu at. % which reached to 57.94 and a lower Ni at. % of 10.99 to give a ratio of Cu/Ni of 5.27 as shown in Table 2 (a). The detection of Cu/Ni with this ratio on the surface confirms the denickelation at this higher potential. On the other hand, from the spectra of Fig. 6(b) the detection of O with higher value of 28.66 at % and Br with lower content of 2.38% confirms that at this potential (1600mV), the dissolution of the alloy not only by general form as a result of the partial current density recorded ($20\text{mA}/\text{Cm}^2$) but also by pitting where the surface had sustained pitting initiation.

From the above result, two types of pitting corrosion were identified at 2 and 4 M LiBr, the first one was recorded after the passive current formation (I_{p1}) while the second at higher anodic polarization potential nearly after 1000mV which occur beside the general dissolution through the recorded partial passive current. Except for the concentrations of 2 and 4M LiBr, the first one of pitting which recorded after the formation of I_{p1} were observed beside the general attack through the partially soluble $\text{Cu}_2(\text{OH})_3\text{Br}$ and the second type of pitting was disappeared. The above results of the formation of the first type of pitting, which recorded after I_{p1} , were further supported by perform a PCP of Cu/30Ni in fresh solution of 6M liBr Fig.7(a), after which the test coupon was changed for a new one and the PCP was done again as shown in Fig.7 (b). Figure 7 (b) indicated that after this procedure the curve displayed a large hysteresis loop and an increase in the length of the passive region. These confirmed the formation of this type of pitting and can be explained by the increase in the negatively charged cation vacancy created by Cu in the p-type semiconductor Cu_2O . These observations can be explained by the increase in passive region thickness, which becomes protective in comparison with the other PCP studied.

The above result of surface analysis is supported by the solution analysis which represents the second side of the coin. Atomic absorption spectrophotometry (A.A.S) is a highly sensitive technique to complement analysis in the corroding medium. Table 2 (b) presents the amount of Cu and Ni

dissolved in 2 M LiBr solution as a result of potentiostatic current –time of Cu/30 Ni electrode at different constant potential of -200, +300 and 1600 mV for 120 min as estimated by A. A. S . The detection of Ni in solution with a ratio lower than that recorded on the surface (Table 2 b), where the Cu/Ni alloy is polarized at -200 mV in 2M LiBr can best be explained as previously discussed where the produced amount of Ni^{++} is expected to be not enough and can be just sufficient to occupy the vacancy created by Cu in the p-type semiconductor Cu_2O . This affects the amount of Ni which can be go to the solution.

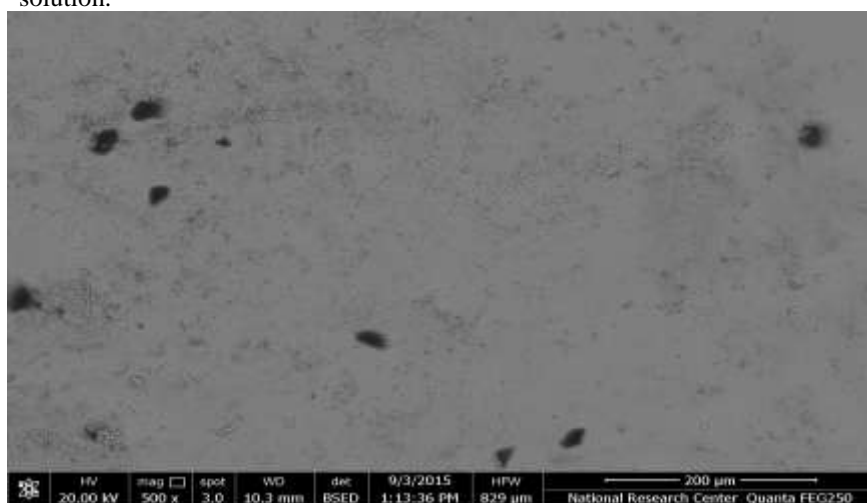


Fig. 6(a)

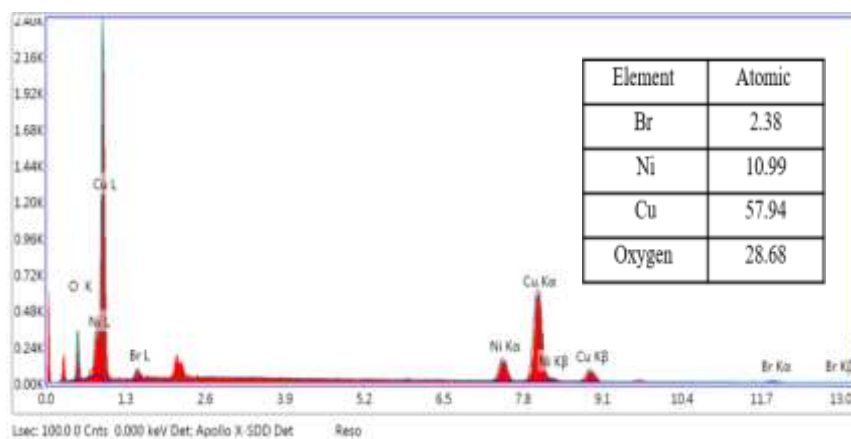


Fig. 6(b)

Fig.6. SEM micrograph of Cu/30Ni electrode obtaining after Potentiostatic current-time of Fig. 3(c)

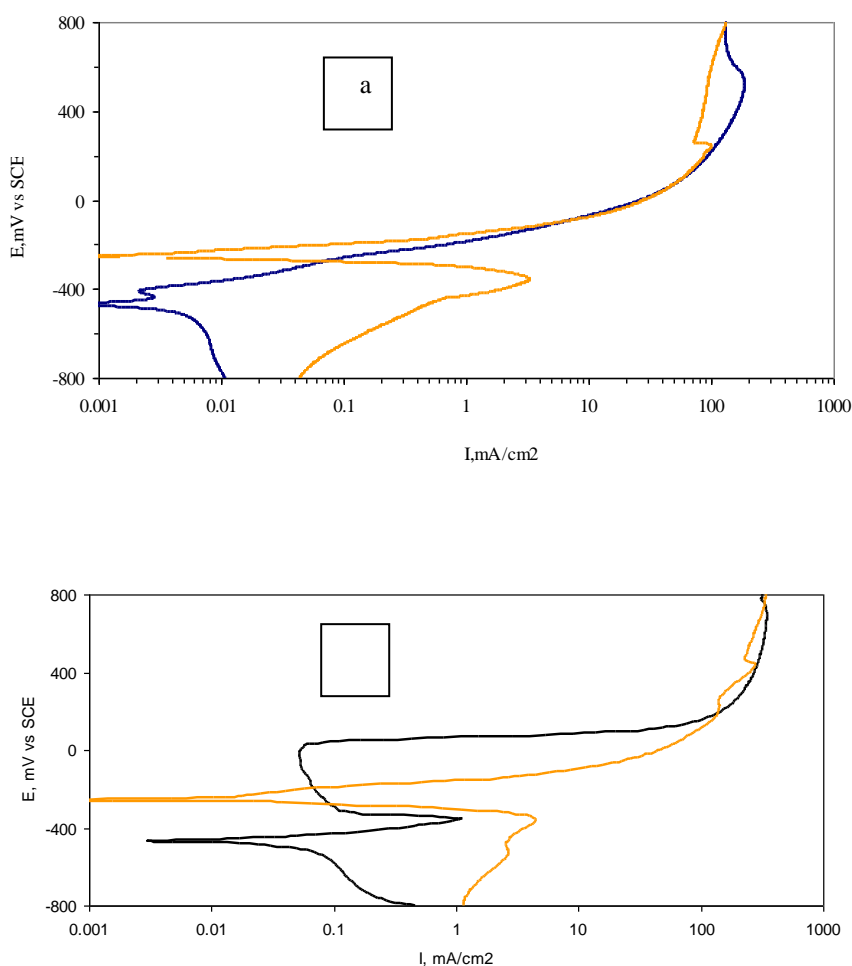


Fig.7. PCP curves of Cu/30Ni in 6 M LiBr (a) New sample and Fresh solution (b) New sample and the solution of experiment (a).

At 300 mV, according to the results included at this potential, $\text{Cu}_2(\text{OH})_3\text{Br}$ is detected on the surface as described in eq 9. On the other hand, the data of A.A.S of Table 2 (b) represent a slight decrease in Ni which is due to the formation of Cu as partially soluble $\text{Cu}_2(\text{OH})_3\text{Br}$ which can restrict the rate of dissolution of Ni.

At 1600 mV, the ratio of Cu/Ni in solution ,Table 2 (b) found to be favour of Ni compared to the alloy surface and alloy bulk composition .This confirms the denickification phenomenon .

TABLE 2(a). EDX analysis of Cu/30Ni electrode obtaining after potentiostatic current-time in 2MLiBr,at the end of Fig.3 .

Potential,mV (SCE)	Cu %	Ni %	O %	Br	Cu/Ni ratio
-200	22.33	14.6	62	1.07	1.52%
+300	45.95	4.01	30.86	19.8	11.45%
-1600	57.95	10.99	28.68	2.38	5.27%

TABLE 2(b). A.A.S. analysis of the solution obtaining after potentiostatic current-time in 2MLiBr, at the end of Fig.3.

Potential, mV (SCE)	Cu%	Ni%	Cu/Ni
-200	78	22	3.34
+300	72	28	2.57
+1600	67	33	2.03

Conclusion

- 1- PCP curves of Cu/30Ni alloy in 2M LiBr exhibit an anodic passivation current which is recorded at low noble anodic potential $\approx -200\text{mV}$ as a result of the formation of a doped Cu_2O . On the other hand Ni from alloy segregates to the formed Cu_2O barrier layer and incorporates into cationic vacancies leading to increase its corrosion resistance and the surface becomes containing more Ni than copper.
- 2- At higher potential $\geq 300\text{ mV}$, after E_{max} , a partially passive film of $\text{Cu}_2(\text{OH})_3\text{Br}$ is formed and the surface contains more Cu than Ni (denickification)
- 3- Solution analysis confirmed the surface analysis where the higher at. % recorded of Cu on the surface shows a corresponding lower ratio in solution and also for Ni and vice versa.
- 4- Two types of pitting were observed only at 2 and 4 M LiBr. Other concentrations of lower or higher LiBr only the first one of pitting were recorded at higher anodic current and general dissolution through the partially soluble $\text{Cu}(\text{OH})_3\text{Br}$ takes place.

References

1. El Meleigy , A.E., Shehata, M.F, Youssef , G.I., Abd El Hamid , Sh. E.and Elwarraky, A.A., Role of Li on the pitting corrosion of copper in LiBr solution. *Ochrona Przed Korozią*, **55** , 10 (2012).

2. **Bustos, E.S.**, *Corros.Sci.*, **51**(5), 1107 (2009).
3. **Igual - Munoz, M.A.** et al, *Corros.Sci.* , **46**(12), 2955 (2004).
4. **Oleink, V., Yn, I.K. and Vartapetyan, A.R.**, *Protect Metals*, **39**(1), 12, (2003).
5. **Gareia-Gareia, D.M.** et al, *Corros.Sci.* **48**(2), 2380 (2006).
6. **Youssef, G.I, Shehata, M.F., El Meleigy, A.A. and El Warraky, A.A.**, Corrosion and corrosion fatigue behaviour of Al-bronze in LiBr solutions. *Ochrona Przed Korozia*, **56** (2), 34 (2013)
7. **El Meleigy, A. E., Abd El Hamid, Sh. E. and El Warraky A. A.**, Corrosion behaviour of copper in LiBr solutions: Effect of temperature, *British Journal of Applied Science & Technology*, **11**(4), 1-18 (2015).
8. **El Meleigy, A.E., Abd Elhamid, Sh.E. and El Warraky, A.A.**, Corrosion behaviour of copper in LiBr solutions-surface examination. *Materialwissenschaft und Werkstofftechnik* , **46**, 59 (2015).
9. **Khalifa, O.R.M., Abd Elhamid, Sh.E. , El Meleigy, A.E., Shehata, M.F. and El Warraky, A. A.**, Corrosion behaviour of copper in LiBr solutions . *Journal of Scientific Research for Science*, **30** (2013).
10. **Saber, T.M.H. and El Warraky , A.A.** , *Br. Corros.J.*, **26**, 279 (1991).
11. **Saber , T.M.H. and El Warraky , A.A.**, *Desalination*, **93**, 473 (1993).
12. **Saber, T.M.H. and El Warraky, A.A.**, *16th Annual Conf. Corrosion Problems in Industry, Hurghada* , Egypt , vol.II, 29 (1997).
13. **Saber, T.M.H. and El Warraky, A.A.**, *17th Annual Conf. Corrosion Problems in Industry, Zafarana* , Egypt , vol.I , 19 (1998).
14. **El Warraky, A.A.**, *Br. Corros .J.* **32**, 57 (1997).
15. **Urzua, R., Siqueiros, J., Morales, L., Rosales, I. and Uruchurtu, J.**, On-line corrosion monitoring of 70 Cu 30 Ni alloy in a LiBr solution under absorption heat pump flow conditions. *Portugaliae Electrochimica Acta*, **27** , 127-142 (2009).
16. **Badawy, W.A., El Rabiee, M., Helal, N.H. and Nady, H.**, The role of Ni in the surface stability of Cu-Al-Ni ternary alloys in sulphate-chloride solutions. *Electrochimica Acta*, **71**, 50-57 (2012).
17. **Ismail, Kh. M., Fathi, Ah.M. and Badawy, W.A** “Electrochemical behaviour of copper-nickel alloys in acidic chloride solutions. *Corro. Sci.* , **48**, 1912-1925 (2006).
18. **Badawy, W.A, Ismail, K.H.M. and Fathi, Ah.M.**, Effect of Ni content on the corrosion behaviour of Cu-Ni alloys in neutral chloride solutions. *Electrochimica Acta*, **50**, 3603-3608 (2005).

19. **Badawy, W.A., Ismail, K.H.M. and Fathi, Ah.M.**, Corrosion control of Cu-Ni alloys in neutral chloride solutions by amino acids. *Electrochimica Acta*, **51**, 4182-4189 (2006).
20. **Milosev, I. and Metikos-Hukovic, M.**, The behaviour of Cu-Ni ($x=10$ to 40 wt%) alloys in alkaline solutions containing chloride ions. *Electrochimica Acta*, **42**, 1537-1548 (1997).
21. **North, R.F. and Pryor, M.J.** *Corros.Sci.*, **10**, 297 (1970).
22. **Shih, H. and Pickering, H.W.**, *J.Electrochem.Soc.* **134**, 1949 (1987).
23. **Kato, C., Ateya, B. G., Castle, J. E. and Pickering, H. W.**, *J. Electrochem. Soc.*, **127**, 1890 (1980).
24. **Kato, C., Ateya, B. G., Castle, J. E. and Pickering, H. W.**, *J. Electrochem. Soc.*, **127**, 1897 (1980).
25. **North, R.F. and Pryor, M.**, *J. Corros. Sci.* **8**, 149 (1968).
26. **Gasparini, R., Della Rocca, C. and Ioannilli, E.**, *Corros. Sci.* **10**, 157 (1970).
27. **Mathiyarasu, J., Paslaniswamy, N and Muralidharan, V.S.**, An understanding of the dissolution and passivation of 70/30 cupronickel alloy. *Indian J. of Chemical Technology*, **9**, 519-525 (2002).
28. **Efird, K. D.**, Potential-PH Diagrams for 90-10 and 70-30 Cu-Ni in sea water. *Corrosion -NACE*, **31**, 77 (1975).
29. **Munoz-Portero, M. J., Garaci-Anton, J., Guinon, J. L. and Perez-Herranz, V.**, "Effect of Bromide Ion Activity on the pourbaix Diagrams for Nickel in concentrated aqueous Lithium Bromide Solutions" *The European Corrosion Congress*, 9-13 sept (2007).
30. **Metiko-Hukovic, M., Babic, R., Skugor, I and Grubac, Z.**, Copper-nickel alloys modified with thin surface films : corrosion behaviour in the presence of chloride ions. *Corros.Sci.* **53**, 347-352 (2011).

(Received
accepted)

دراسة سلوك سبيكة النحاس- نيكل (30/70) في محلول بروميد الليثيوم

علي عبد الفتاح الوراقى ، عبير عصمت المليجي و شيماء عصمت عبد الحميد
قسم الكيمياء الفيزيقيه – المركز القومي للبحوث- الجيزه – مصر .

تمت دراسة سلوك تاكل سبيكة النحاس – نيكل (30-70) في محاليل ذات تركيبات مختلفه من بروميد الليثيوم من تركيز 10^{-1} حتي 9 مولر (9 مولر تعادل 850 جرام/لتر وهو ما يستخدم صناعيا). استخدمت في هذه الدراسه القياسات الكهروكيميائيه مثل طريقه الاستقطاب البنتشوديناميكي الحلقي (PCP) وقياس التغير في التيار مع الزمن باستخدام طريقه الاستقطاب البنتشوستاتيكي بالاضافه الي فحص اسطح العينات الناتجه من الاستقطاب البنتشوستاتيكي باستخدام الميكروسكوب الماسح الالكتروني (SEM) وكذلك الاشعه السينيه المشتهه (EDX) وللوضوح واستكمال الصوره تم تحليل المحاليل الناتجه من الاستقطاب البنتشوستاتيكي ايضا باستخدام الامتصاص الذري الاسبكتروفوتوميترى (A.A.S) اوضحت الدراسه تكوين طبقه ذات حمايه (Passive) عند التيار I_{p1} وعند جهد منخفض جدا 200- مللي فولت وذلك نظرا لتكوين طبقه حاميه من اوكسيد النحاسوز والذي يتخلله عنصر النيكل (doped Cu_2O) وتبين ذلك من وجود النيكل بنسبه اكبر علي السطح منها عن ما هو موجود في السبيكة

بزياده قيمه الجهد الانودي الي اكبر من او تساوي 300 مللي فولت وذلك بعد تكوين قمه (Peak) ويكون التيار عندها اكبر ما يمكن تتكون طبقه لها حمايه جزئيه من $Cu_2(OH)_3Br$ واطهرت تحاليل الاسطح باستخدام EDX نقص نسبه النيكل علي السطح عنه في السبيكة والاكثر من ذلك اوضحت نتائج تحاليل المحاليل باستخدام A.A.S ان نسبه النحاس /نيكل في المحلول تعطي الرؤيه العكسيه لما هو موجود علي السطح مما اعطي رؤيه متكامله لعملية الذوبان من ناحيه اخري اثبتت الدراسات السابقه ظهور نوعين من التاكل الثقبي عند تركيزات 2و4مولر فقط النوع الاول يحدث بعد تكوين طبقه الحاميه عند القيمه الصغيره من التيار I_{p1} والنوع الاخر يظهر عند قيمه عاليه من التيار الانودي تقريبا بعد 1000 مللي فولت اي بعد تكوين طبقه ذات الحمايه الجزئيه من $Cu_2(OH)_3Br$ ما عدا ذلك في المحاليل المركزه او المخففه بعيدا عن 2و4مولر يحدث التاكل الثقبي الاول فقط بجانب حدوث التاكل العام في نفس الوقت.